The effect of vapour cavitation occurrence on the hydrodynamic performance of an intercepted base-ventilated hydrofoil

B.W. Pearce and P.A. Brandner

Australian Maritime College

University of Tasmania, Launceston, Tasmania 7250, Australia

Abstract

Experimental results of the hydrodynamic performance of a novel high-speed hydrofoil concept are presented. The hydrofoil is symmetric, wedge shaped and makes use of a mechanism for producing a forward-facing step on either upper or lower surfaces to induce a ventilated supercavity and produce bi-directional lift. The hydrofoil remains fully-wetted at low incidence with leading edge partial vapourous cavitation and eventual suction side supercavity formation from the leading edge with incidence increase. Cavitation hysteresis as incidence is reduced back from the latter condition is significant. The corresponding detrimental effect on the resulting hydrodynamic performance is presented and shows that there is a practical upper incidence limit, analogous to stall in single phase flow, in the application of this novel hydrofoil concept.

Introduction

A novel design for a base-ventilated supercavitating hydrofoil was conceived by Australian Naval Architect Tony Elms as embodied in the patent application entitled "Improved Hydrofoil Device" [5]. One possible application of this concept is for motion control of high-speed ships where cavitation numbers at which lift generating devices must operate are such that cavitation problems arise on hydrofoils intended for non-cavitating operation, although not low enough for supercavitation to naturally develop. The basis of this concept is the use of a symmetrical hydrofoil section from which a trailing supercavity is formed detaching from geometric discontinuities, located between the mid-chord and trailing edge, on both the upper and lower surfaces, as shown in Figure 1. Deflection of the hydrofoil tail section creates a forward-facing step (FFS) on one side and a backward-facing step (BFS) on the other. The use of such a FFS on the trailing edges of lifting surfaces or transoms of ship hulls are often termed spoilers or interceptors. Flow asymmetry created by the discontinuities may thus be used to create bi-directional lift as required for vessel motion control from a hydrofoil at nominally zero incidence. Various mechanisms for venting of the incondensable gas are possible including ducting of atmospheric air via struts supporting the hydrofoil or via ports on the base of the leading or trailing sections of the hydrofoil.
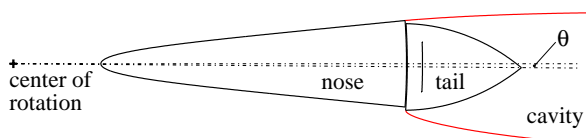
Figure 1: Concept hydrofoil design for production of bi-directional lift intended to operate with a ventilated supercavity detaching from discontinuities generated by articulating the trailing hydrofoil section.

Considerations in the design and optimisation of this system include the hydrofoil section geometry, the means for venting of the incondensable gas and the required flow to maintain the supercavity. The design of the leading hydrofoil section involves optimising lift and drag and incidence tolerance as it relates to flow separation, leading edge vapourous cavitation and potential for the ventilated supercavity to transition to the leading edge on the low pressure side.

For the purposes of the present work only the leading section of the hydrofoil is considered with the FFS or interceptor produced by adding a flat vertical sharp-edged plate to the hydrofoil base. Basic parameters of interest include the leading edge radius, thickness to chord ratio and trailing edge slope. To maintain cavity detachment from the trailing edge the flow over the full length of the hydrofoil must remain attached. Apart from aspects particular to the leading edge ([3]) separation is avoided if a favourable pressure gradient is maintained to the trailing edge. This is achieved if the section thickness and hence first and second derivatives vary monotonically from leading to trailing edge.

Suitable section geometries have been developed from the equation for the leading portion of the thickness distribution of the NACA 4-digit-modified-series airfoil [6]. Use of this profile enables both the leading edge radius and the trailing edge slope to be specified for a given thickness to chord ratio. A detailed description of this geometry is given in [7]. A series of 5 physical models have been manufactured based on the results of a comprehensive numerical study into the effect of foil geometry on hydrodynamic performance [7]. Some initial results for the hydrofoil 20-4 are presented as part of the present study (see also [8]). The 20-4 designation for this hydrofoil denotes 20% thickness to chord ratio and $4°$ trailing edge slope.

Experimental overview

Experiments were carried out in the Cavitation Research Laboratory (CRL) water tunnel at the Australian Maritime College (AMC). The tunnel test section is 0.6 m square by 2.6 m long in which the operating velocity and pressure ranges are 2 to 12 m/s and 4 to 400 kPa absolute respectively. The tunnel has ancillary systems for rapid degassing and for continuous injection and removal of nuclei and large volumes of incondensable gas. A detailed description of the facility is given in [1, 2].

The experimental setup has been developed to allow either 2- or 3D testing of the model hydrofoils. For the present work only the 2D case is investigated. To enable a 2D test and to confine the the magnitude of forces to suit the setup a partition is fitted on the test section vertical centreplane. The model was mounted horizontally in the middle window midway along the test section length to avoid any influence on the pressure tappings used to measure the test section static pressure and velocity. The model hydrofoil is mounted on a 6-component force balance to measure the complete hydrodynamic load vector. The hydrofoil incidence may be indexed automatically from a stepper motor

controlled from the data acquisition system.

This arrangement provides for a hydrofoil span of 276 mm (chord of 140 mm) with 0.5 mm clearance between the partition and the end of the model. Details of model hydrofoil are given in Figure 2. The model hydrofoil is machined from solid Aluminium and anodised. The interceptor is formed by attaching a sharp edged plate to the base of the hydrofoil. Several plates are available to test the effect of the interceptor height on the hydrofoil performance. Only one interceptor, of height 1% of the chord, was tested for the present work. The venting air is introduced through 6 holes on the base centreline equispaced along the span. A tube routed through the ventilation manifold extending into the cavity enables measurement of the cavity pressure and hence the ventilated cavitation number as described, along with a more detailed explanation of the experimental setup and method used, in [8].
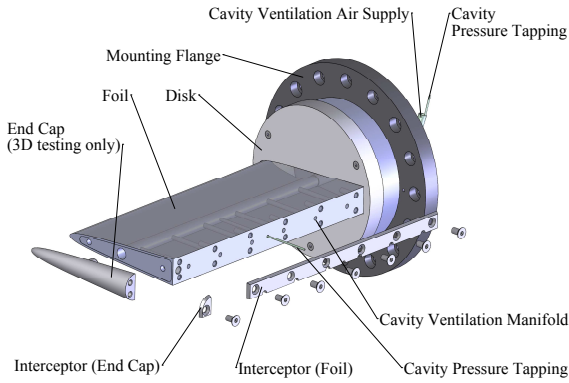
Figure 2: Exploded view of typical model hydrofoil.

Two cavitation numbers are required to characterise the present problem in which both vapour and ventilated cavities occur, $\sigma_v = (p - p_v)/0.5\rho U^2$ and $\sigma_c = (p - p_c)/0.5\rho U^2$ where σ_v and σ_c are the cavitation numbers for the vapour and ventilated cavities respectively, p is the freestream static pressure, p_v the vapour pressure, p_c the pressure within the ventilated cavity, ρ the density and U is the freestream velocity. Hydrofoil vapour cavitation numbers typical for high-speed ship motion control vary between about 0.5 to 1.0 and hence σ_v values of 0.5, 0.75 and 1.0 were chosen for testing. The value of σ_c is controlled by the ventilation flow rate as well as σ_v. For each of the σ_v values ventilation flow rates were chosen to create a cavity of about 10 chord lengths at low incidence and to maintain a supercavity at high incidences (see Table 1).

Typical incidence excursions for hydrofoils used for high-speed ship motion control are estimated to be about +/- 2.5° [4]. However, larger angles may occur in extreme conditions and an objective of the present work is to investigate limiting behaviour of this hydrofoil concept and therefore tests where carried out until leading edge vapour cavitation occurred and the ventilated cavity transitioned to the leading edge on the low pressure side. Depending on the range tested the hydrofoil incidence was indexed in either 0.2° or 0.25° increments. For all the hydrofoil tests the incidence was indexed through a complete cycle of negative and positive values to show any hysteresis or gravity effects. All tests were carried out at a Reynolds number of 1.4×10^6 (based on chord and freestream velocity).

Results and discussion

Results are presented for the hydrofoil with an interceptor of 1% chord at three σ_v values (0.5, 0.75 and 1.0) and three corresponding σ_c values (0.15, 0.19, and 0.22) at each σ_v. The values

of σ_c were obtained by vaying the ventilation air rate between 52 and 500 SLPM as listed in Table 1. The ventilation flow rate is given as a mass flow rate, Q_m, in Standard Litres per Minute (SLPM). The volume flow coefficent, C_{Qv}, is given by Q_v/stU where the volume flow, Q_v, has been calculated from Q_m, s is the span, t the base thickness including the interceptor and U is the free stream velocity. The hydrofoil incidence was varied over a cycle from $-4°$ up till, or past, max lift (stall) and back down to $-4°$. The data is shown in Figures 3, 4 and 5. The measured lift and drag are non-dimensionalised as $C_L = L/0.5\rho U^2 A$ and $C_D = D/0.5\rho U^2 A$ where the reference area, A is the span x chord. Figure 3 shows the lift curve for a single σ_c with photos of cavitation occurrence to demonstrate general behaviour. Figure 4 shows typical plots of both the lift and drag coefficients, up to $+1°$ past stall, as a function of incidence and σ_v (for $\sigma_c = 0.19$).

σ_v	σ_c	Q_m (SLPM)	C_{Qv}	
0.5	0.18	100	0.11	
0.75	0.19	200	0.13	Fig. 4
1	0.19	300	0.14	
0.5	0.15	135	0.12	
0.5	0.19	100	0.10	
0.5	0.22	52	0.06	
0.75	0.15	310	0.17	
0.75	0.19	200	0.12	Fig. 5
0.75	0.22	144	0.09	
1	0.15	500	0.19	
1	0.19	300	0.12	
1	0.23	230	0.10	

Table 1: Test parameters.

For the case of $\sigma_v = 0.75$ shown in Figure 3 no leading edge cavitation was observed to occur below about 1.5° regardless of the direction of incidence change (showing the slight change of slope in the lift curve below about 2 deg to be due to viscous effects). The photo at zero incidence shows only the ventilated supercavity detaching from the hydrofoil trailing edge on the upper, low pressure, surface and the interceptor on the lower, high pressure, surface. For increasing incidence leading edge vapour cavitation inception occurs at about 2.5°. This cavity grows with incidence increase reaching maximum lift at about 4° where the cavity length is about half the chord. With further incidence increase the lift reduces suddenly with the transitioning of the ventilated cavity detachment to the leading edge. Any further increase in incidence only achieves modest lift increase since only the lower surface is able to contribute to lift increase. To eliminate the leading edge cavity the incidence must be returned to about 1.5°, that is, a value below that for inception of leading edge cavitation for increasing incidence. The photos show the breakup of the leading edge into streaks that are slowly eliminated with incidence reduction after which the forces return to those of the original lift curve.

Similar behaviour and hysteresis from cavitation was observed for all the cases tested as shown in Figure 4. These results also show how the both the lift and drag change with the formation of the leading edge vapour cavitation and the transition of the ventilated cavity to the leading edge. Regardless of the σ_v value the lift slope for the fully wetted flow is the same in all cases. A decrease in σ_v, reduces both the maximum lift obtained and the incidence at which it occurs. The incidence at which leading edge cavitation is extinguished is shown however to be independent of σ_v. The ventilation rate is also shown to have little effect on the resulting hydrodynamic performance as shown in
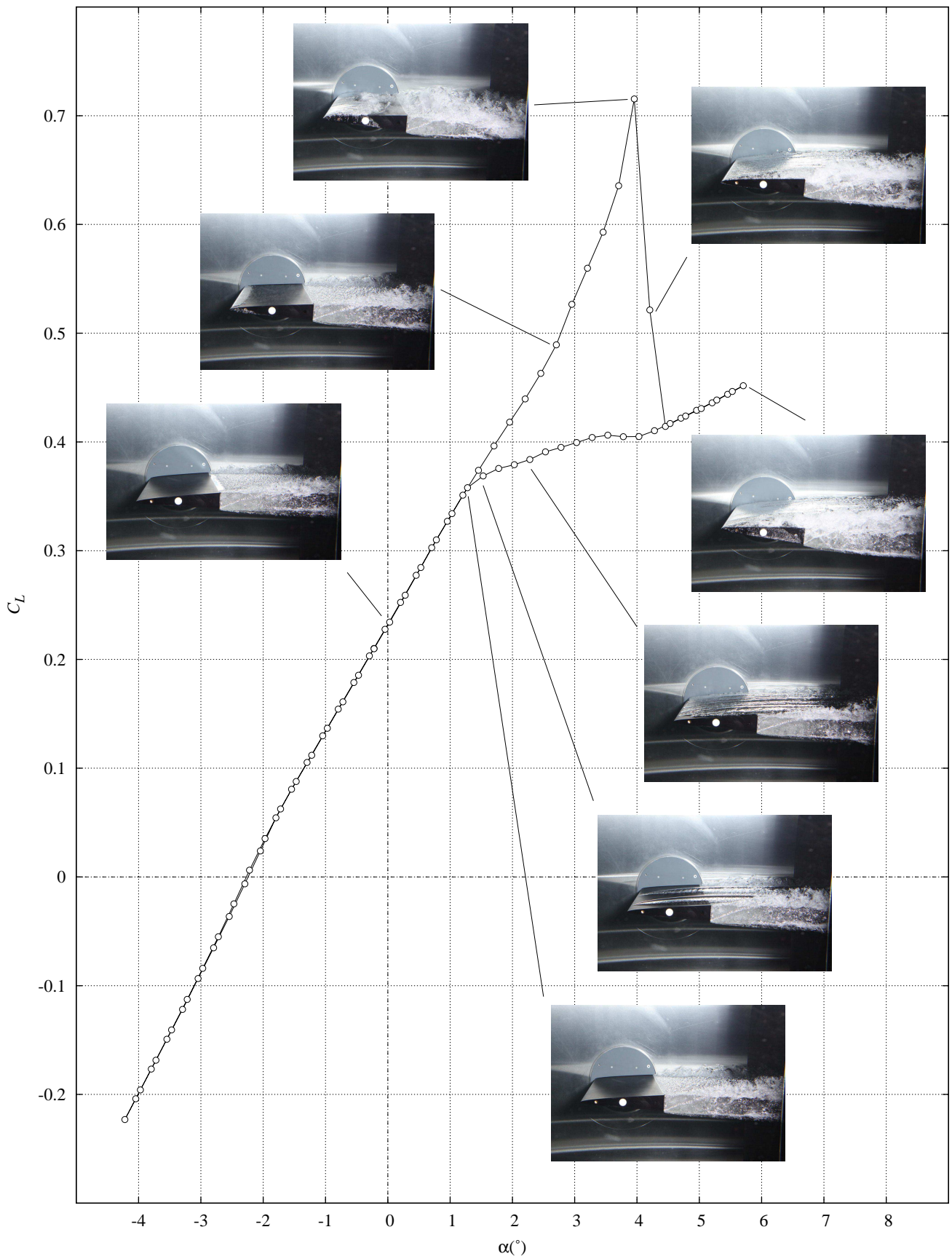
Figure 3: Lift curve for 2D test of the 20-4 hydrofoil profile with an interceptor of height 1% chord fitted at a vapour cavitation number of 0.75, ventilated cavitation number of 0.19 and Reynolds number of 1.4×10^6. Photos show cavitation occurrence and its influence on the lift curve shape and hysteresis.

Figure 5. Here, the incidence is cycled up to just below stall and then back down showing no cavitation hysteresis if the leading edge natural cavitation does not transition to a leading edge supercavity. Also evident is that the ventilation flow rate has nominally no effect on the lift produced in the fully wetted regime.
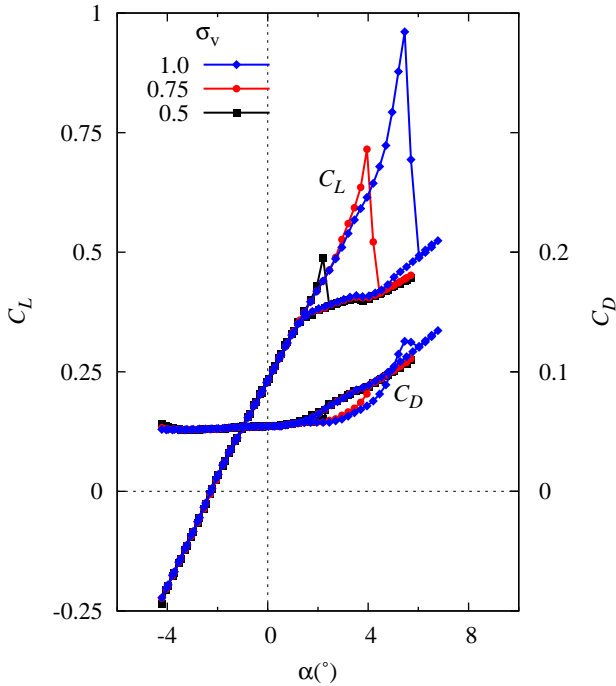
Figure 4: 2D lift and drag data for an incidence cycle up to past stall and back down showing cavitation hysteresis. For the 20-4 hydrofoil profile with an interceptor of height 1% chord at σ_v of 0.5,0.75 & 1.0, $\sigma_c = 0.19$ and Reynolds number of 1.4×10^6.

Conclusions

An experimental setup has been developed to investigate the capabilities of ventilated supercavitating hydrofoils for parameters suitable for devices used for motion control of high-speed ships. Initial results obtained for a novel hydrofoil concept show the device has potential for application in high-speed ship motion control where incidence tolerances of only a few degrees are required. The use of an interceptor for lift modulation rather than hydrofoil incidence shows promise in this application. Although high lift and lift/drag are possible at higher incidences the flow becomes unsteady as leading edge vapour cavities form and interact with the base ventilated supercavity. With ongoing incidence increase the ventilated supercavity ultimately transitions to the leading edge with subsequent rapid loss of lift from the unwetting of the low pressure side. In the incidence range below the formation of leading edge natural cavitation neither the vapour nor the ventilated cavitation numbers has an effect on the resulting hydrodynamics performance. The limiting incidence value corresponding to maximum lift is a function of the vapour cavitation number but is insensitive to the rate of ventilation, i.e. the ventilated cavitation number. There also was found to be no cavitation hysteresis if leading edge natural cavitation dose not transition to a supercavity.

Acknowledgements
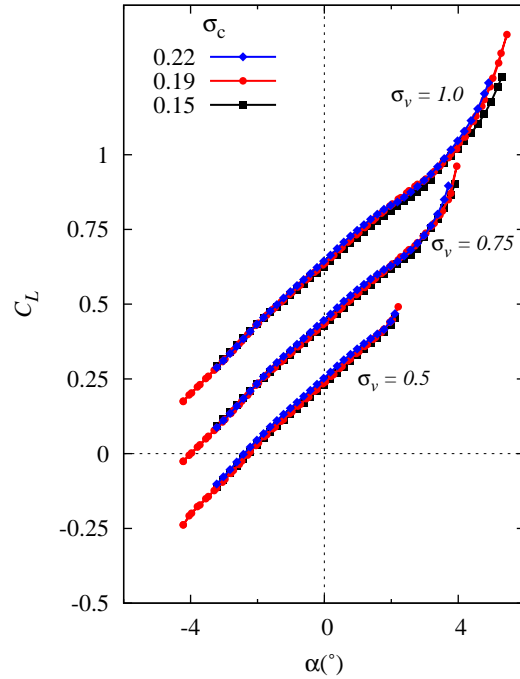
Figure 5: 2D lift data for an incidence cycle up to just before stall and back down showing the absence of cavitation hysteresis in this case. For the 20-4 hydrofoil profile with an interceptor of height 1% chord at σ_v of 0.5, 0.75 & 1.0, σ_c of 0.15, 0.19 and 0.22 and Reynolds number of 1.4×10^6. The data for each value of σ_v are shown as a staggered plot offset by 0.2.

References

[1] Brandner, P. A., Lecoffre, Y. and Walker, G. J., Development of an Australian National Facility for cavitation research, in *Sixth International Symposium on Cavitation - CAV2006*, MARIN, Wageningen, The Netherlands, 2006.

[2] Brandner, P. A., Lecoffre, Y. and Walker, G. J., Design considerations in the development of a modern cavitation tunnel, in *16th Australasian Fluid Mechanics Conference*, Crown Plaza, Gold Coast, Australia, 2007, 630–637.

[3] Davis, M., Design of flat plate leading edges to avoid flow separation, *AIAA Journal*, **18**, 1980, 598–600.

[4] Elms, A., Personal communication, 2003.

[5] Elms, A. R., Improved hydrofoil device, *International Patent Number* WO 99/57007, World Intellectual Property Organisation, 1999.

[6] Ladson, C. L., Brooks, C. W., Hill, A. S. and Sproles, D. W., Computer program to obtain ordinates for NACA airfoils, Technical Memorandum 4741, NASA, 1996.

[7] Pearce, B. W., *Ventilated supercavitating hydrofoils for ride control of high-speed craft*, Ph.D. thesis, University of Tasmania, 2011.

[8] Pearce, B. W. and Brandner, P. A., Experimental investigation of a base-ventilated supercavitating hydrofoil with interceptor, in *8th International Symposium on Cavitation, Cav2012*, Singapore, 2012, Paper No. 218.